Supplement of Atmos. Chem. Phys. Discuss., 14, 19791–19835, 2014
http://www.atmos-chem-phys-discuss.net/14/19791/2014/
doi:10.5194/acpd-14-19791-2014-supplement

Atmospheric Chemistry and Physics
Discussions
Open Access

Supplement of

Elemental ratio measurements of organic compounds using aerosol mass spectrometry: characterization, improved calibration, and implications

M. R. Canagaratna et al.

Correspondence to: M. R. Canagaratna (mrcana@aerodyne.com)

Supplementary Figures

S1: a) Standard deviations in repeated elemental ratio measurements of several standards obtained with a single instrument. Standard deviations are shown for O:C and H:C ratios calculated with the Aiken-Ambient method. b) Scatter plots of Aiken-Ambient O:C ratios calculated for several standards with three different AMS instrument (AMS_1, AMS_2, and AMS_3. c) Scatter plots of Aiken-Ambient H:C ratios calculated for several standards with three different AMS instrument (AMS_1, AMS_2, and AMS_3).

S2: Vaporizer temperature dependence of the fractional AMS ion intensity measured for CO_2^+, CO^+, and H_2O^+ for some of the standards measured in this study. For each standard, fractional ion intensities measured at 600^oC (first bar) and 200^oC (second bar) are shown.

S3: Scatter plots of key ions observed in the AMS spectra of laboratory standards. Panel a shows OH^+ vs. H_2O^+, panel b shows O^+ vs. H_2O^+, and panel c shows O^+ vs. CO_2^+. The dashed line denotes the default relationships assumed when analyzing AMS data with the Aiken-Ambient method.

S4: Dependence of the fractional CHO^+ ion intensity on functional composition of OA standards. The standards are separated into two groups according to those that contain at least one -OH or -OR functional group and those that don't contain any of those functional groups.

S5: a) Scatter plot between OM/OC values calculated with Improved-Ambient method and the known OM/OC values for standard molecules. b) Scatter plot between OM/OC values and O:C values calculated with the Improved-Ambient method for standard molecules. The black line shows a linear fit through the data.

Figure S1

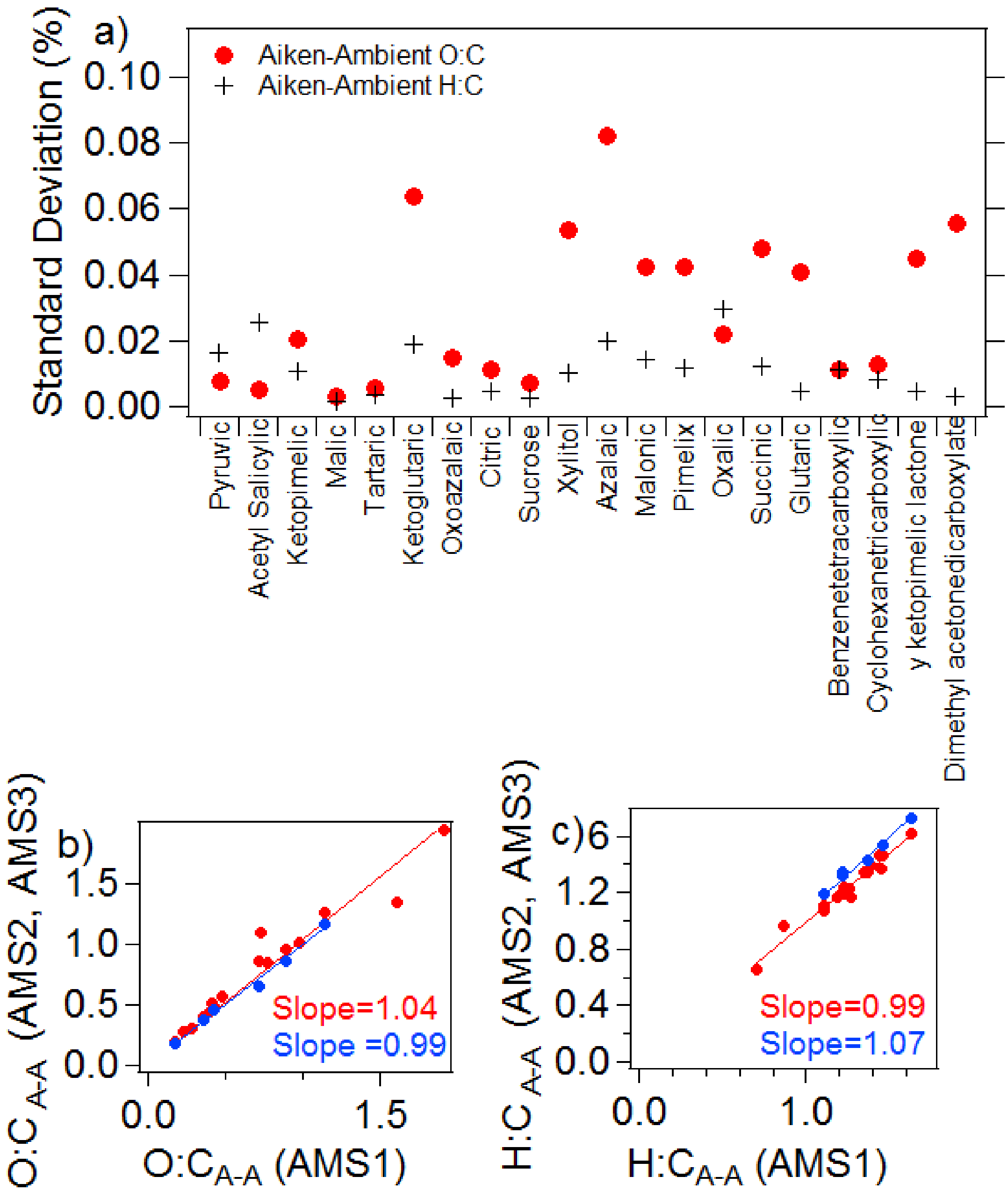

a)
Standard Deviation (%)
0.10
0.08
0.06
0.04
0.02
0.00
Aiken-Ambient O:C
Aiken-Ambient H:C
Pyruvic
Acetyl Salicylic
Ketopimelic
Malic
Tartaric
Ketoglutaric
Oxoazalaic
Citric
Sucrose
Xylitol
Azalaic
Malonic
Pimelix
Oxalic
Succinic
Glutaric
Benzenetetracarboxylic
Cyclohexanetricarboxylic
y ketopimelic lactone
Dimethyl acetonedicarboxylate
b)
O:C A-A (AMS2, AMS3)
1.5
1.0
0.5
0.0
Slope=1.04
Slope =0.99
0.0
1.5
O:C A-A (AMS1)
c)
H:C A-A (AMS2, AMS3)
6
1.2
0.8
0.4
0.0
Slope=0.99
Slope=1.07
0.0
1.0
H:C A-A (AMS1)

Figure S2

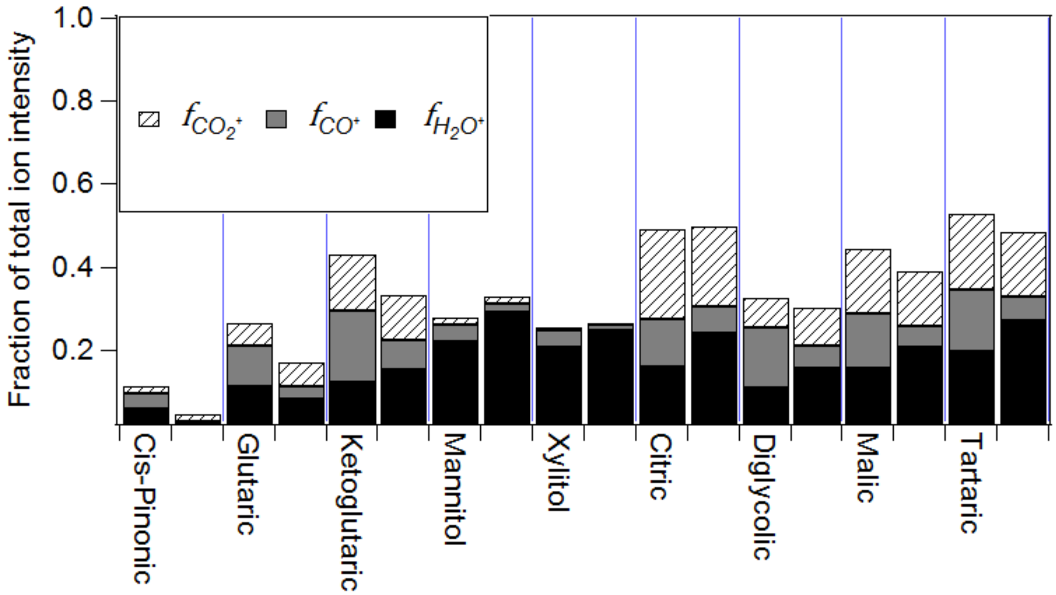

Fraction of total ion intensity
1.0
0.8
0.6
0.4
0.2
$f_{CO_2^+}$
f_{CO^+}
$f_{H_2O^+}$
Cis-Pinonic
Glutaric
Ketoglutaric
Mannitol
Xylitol
Citric
Diglycolic
Malic
Tartaric

Figure S3

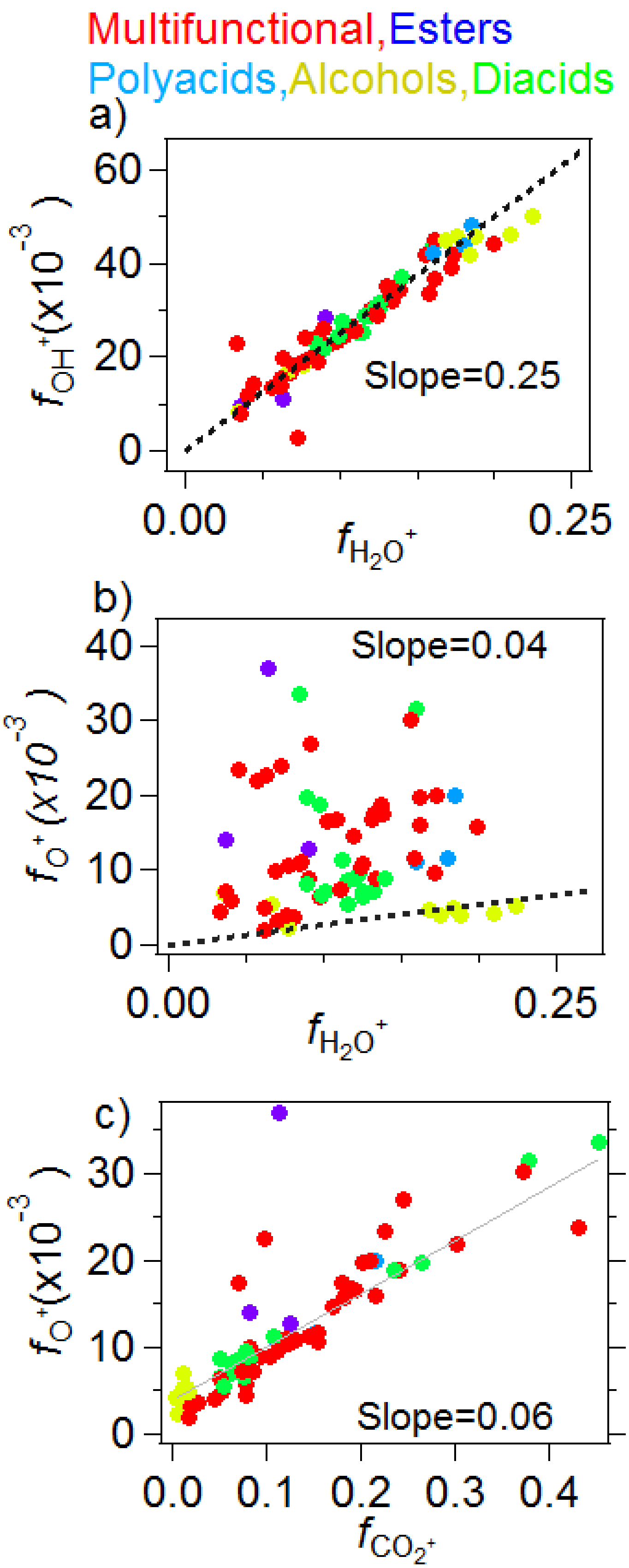

Multifunctional,Esters
Polyacids,Alcohols,Diacids
a)
Slope=0.25
b)
Slope=0.04
c)
Slope=0.06

Figure S4

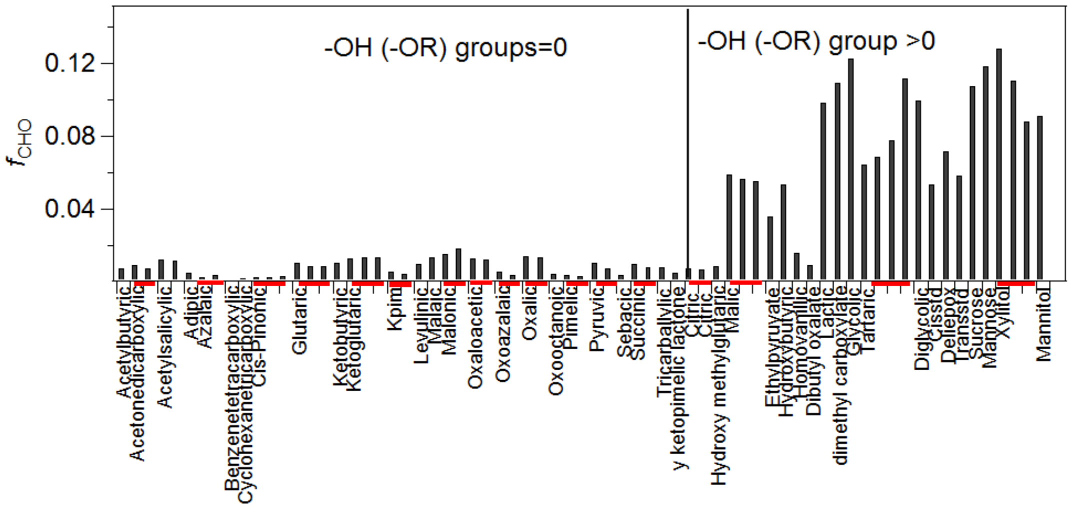

-OH (-OR) groups=0
-OH (-OR) group >0
0.12
0.08
0.04
f_{CHO}
Acetylbutyric
Acetonedicarboxylic
Acetylsalicylic
Adipic
Azalaic
Benzenetetracarboxylic
Cyclohexanetricarboxylic
Cis-Pinonic
Glutaric
Ketobutyric
Ketoglutaric
Kpim
Levulinic
Malaic
Malonic
Oxaloacetic
Oxoazalaic
Oxalic
Oxooctanoic
Pimelic
Pyruvic
Sebacic
Succinic
Tricarballylic
y ketopimelic lactone
Citric
Citric
Hydroxy methylglutaric
Malic
Ethylpyruvate
Hydroxybutyric
Homovanillic
Dibutyl oxalate
Lactic
dimethyl carboxylate
Glycolic
Tartaric
Diglycolic
Cisstd
Deliepox
Transstd
Sucrose
Mannose
Xylitol
Mannitol

Figure S5

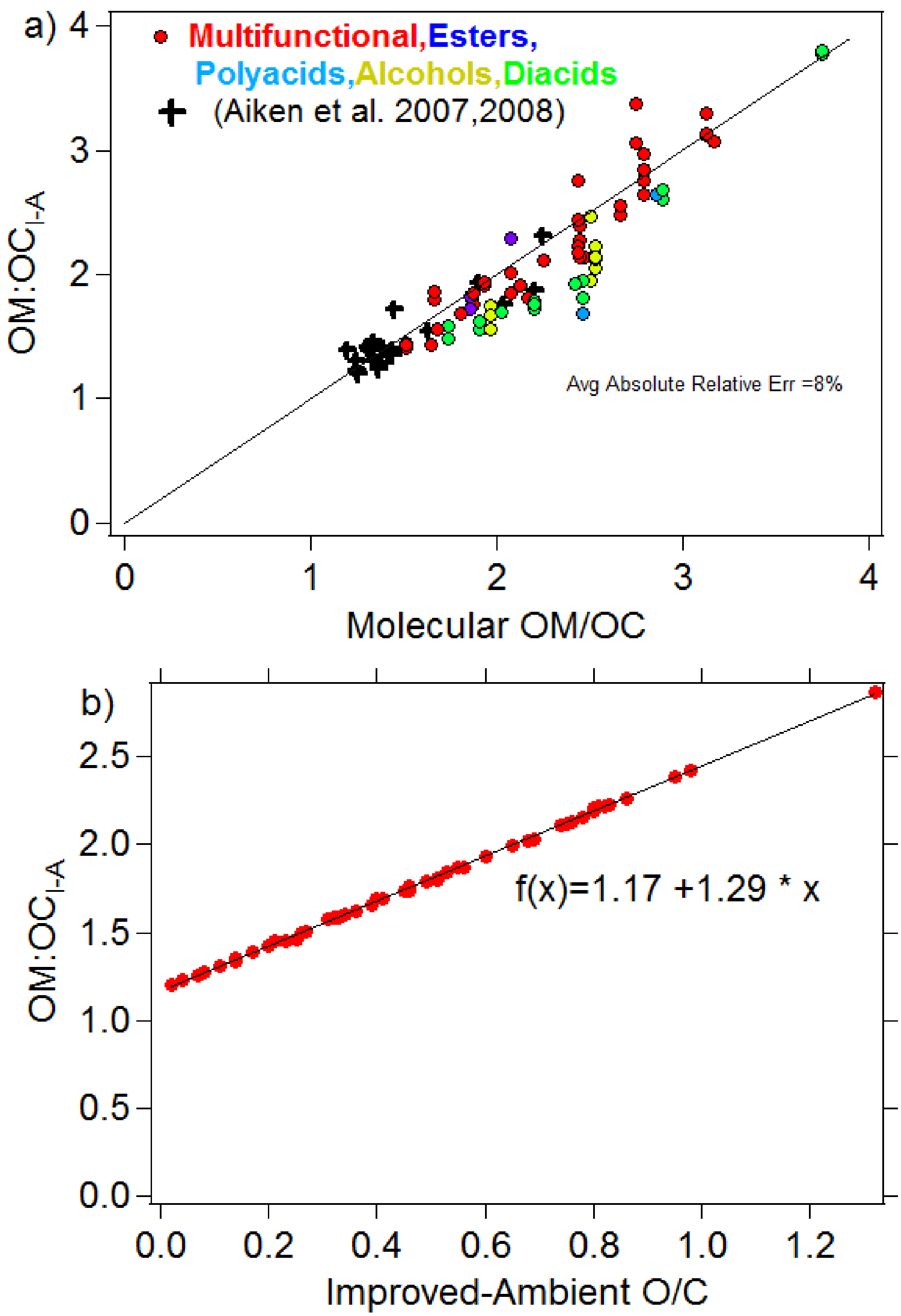
a)
Multifunctional,Esters,
Polyacids,Alcohols,Diacids
(Aiken et al. 2007,2008)
Avg Absolute Relative Err =8%
OM:OC$_{I-A}$
Molecular OM/OC
b)
f(x)=1.17 +1.29 * x
OM:OC$_{I-A}$
Improved-Ambient O/C

Table S1. Improved-Ambient (I-A) results for previously reported ambient OA components.

Ambient PMF components	Reference	O:C $_{I-A}$	Change (%)	H:C $_{I-A}$	Change (%)	OM:OC$_{I_A}$	Change (%)	$\overline{OS}_{C\ (I-A)}$	Absolute Change
HOA	(Aiken et al., 2009)	0.21	31	2.03	10	1.45	6	-1.61	-0.09
	(DeCarlo et al., 2010)	0.07	24	1.92	7	1.26	2	-1.77	-0.10
	(Docherty et al., 2011)	0.02	26	2.10	7	1.21	2	-2.05	-0.13
	(Ge et al., 2012)	0.11	27	1.95	8	1.33	3	-1.72	-0.10
	(Gong et al., 2012)	0.11	26	1.94	8	1.34	3	-1.71	-0.09
	(He et al., 2011)	0.14	25	1.83	8	1.35	4	-1.55	-0.07
	(Wang et al., 2010)	0.14	28	1.88	9	1.34	4	-1.60	-0.09
	(Huang et al., 2012)	0.20	28	1.93	9	1.43	5	-1.52	-0.07
	(Huang et al., 2013) (Winter)	0.14	29	2.02	9	1.38	4	-1.74	-0.11
	(Huang et al., 2013) (Summer)	0.17	29	1.93	9	1.40	5	-1.60	-0.09
	(Mohr et al., 2012)	0.04	26	2.10	7	1.23	2	-2.03	-0.13
	(Saarikoski et al., 2012)	0.26	24	1.84	8	1.50	5	-1.32	-0.03
	(Setyan et al., 2012)	0.11	34	1.99	11	1.31	4	-1.77	-0.14
	(Sun et al., 2011)	0.08	26	1.96	7	1.26	3	-1.81	-0.10
BBOA	(Aiken et al., 2009)	0.40	34	1.88	11	1.69	10	-1.08	0.01
	(DeCarlo et al., 2010)	0.55	31	1.60	12	1.88	11	-0.49	0.09
	(Ge et al., 2012)	0.46	40	1.78	14	1.79	12	-0.86	0.04
	(Gong et al., 2012)	0.25	31	1.55	10	1.50	6	-1.05	-0.02
	(He et al., 2011)	0.45	42	1.69	15	1.81	12	-0.79	0.04
	(Huang et al., 2011)	0.34	32	1.79	10	1.60	8	-1.10	0.00
	(Huang et al., 2013) (Winter)	0.36	35	1.70	12	1.66	9	-0.97	0.00
	(Mohr et al., 2012)	0.31	30	1.94	10	1.58	8	-1.31	-0.02
	(Saarikoski et al., 2012)	0.33	44	1.77	16	1.59	11	-1.11	-0.04
COA	(Ge et al., 2012)	0.14	27	1.85	8	1.35	4	-1.57	-0.07
	(Wang et al., 2010)	0.14	28	1.88	9	1.34	4	-1.60	-0.09
	(Mohr et al., 2012)	0.27	31	1.73	10	1.51	7	-1.18	-0.03
	(Sun et al., 2011)	0.23	26	1.71	8	1.44	5	-1.26	-0.04
OOA	(Aiken et al., 2009) (OOA)	0.80	33	1.67	14	2.20	15	-0.07	0.20
	(DeCarlo et al., 2010) (SVOOA)	0.83	29	1.46	13	2.23	13	0.20	0.21
	(DeCarlo et al., 2010) (LVOOA)	1.32	29	1.29	16	2.87	17	1.34	0.42
	(Docherty et al., 2011) (SV-OOA)	0.32	40	1.88	14	1.59	10	-1.23	-0.04
	(Docherty et al., 2011) (LVOOA)	0.86	20	1.40	10	2.26	10	0.32	0.16
	(Ge et al., 2012) (OOA)	0.55	31	1.60	12	1.88	11	-0.50	0.09
	(Gong et al., 2012) (SV-OOA)	0.46	25	1.46	10	1.75	8	-0.53	0.06
	(Gong et al., 2012) (LV-OOA)	0.68	24	1.43	10	2.06	10	-0.06	0.14
	(He et al., 2011) (SV-OOA)	0.60	32	1.64	13	1.95	12	-0.45	0.10
	(He et al., 2011) (LV-OOA)	0.76	29	1.43	14	2.17	12	0.09	0.17
	(Wang et al., 2010) (OOA1)	0.56	17	1.48	7	1.87	7	-0.35	0.07
	(Wang et al., 2010) (OOA2)	0.65	38	1.54	16	1.99	15	-0.24	0.15
	(Huang et al., 2011) (SV-OOA)	0.49	27	1.63	10	1.79	9	-0.64	0.06
	(Huang et al., 2011) (LV-OOA)	0.80	26	1.45	11	2.19	12	0.16	0.18
	(Huang et al., 2012) (SV-OOA)	0.45	30	1.65	12	1.74	10	-0.74	0.04
	(Huang et al., 2012) (LV-OOA)	0.81	25	1.66	11	2.22	11	-0.04	0.15
	(Huang et al., 2013) (Winter; OOA)	0.75	28	1.45	12	2.16	12	0.06	0.17
	(Huang et al., 2013) (Summer; OOA)	0.53	28	1.63	11	1.86	10	-0.58	0.07
	(Mohr et al., 2012) (SV-OOA)	0.41	29	1.75	11	1.70	9	-0.92	0.02
	(Mohr et al., 2012) (LV-OOA)	0.98	31	1.35	14	2.42	16	0.62	0.30
	(Saarikoski et al., 2012) (OOAa)	0.95	20	1.46	10	2.39	10	0.44	0.19
	(Saarikoski et al., 2012) (OOAb)	0.80	28	1.58	12	2.20	13	0.03	0.18
	(Saarikoski et al., 2012) (OOAc)	0.69	21	1.36	9	2.03	9	0.01	0.12
	(Setyan et al., 2012) (LO-OOA)	0.51	21	1.46	8	1.80	7	-0.45	0.06
	(Setyan et al., 2012) (MO-OOA)	0.74	37	1.52	15	2.11	15	-0.04	0.20
	(Sun et al., 2011) (SVOOA)	0.51	33	1.58	13	1.81	11	-0.56	0.08
	(Sun et al., 2011) (LVOOA)	0.78	24	1.43	11	2.16	11	0.14	0.17

Table S2. Improved-Ambient (I-A) results for total OA from previously reported ambient field campaigns.

Reference	$O:C_{I-A}$	Change (%)	$H:C_{I-A}$	Change (%)	$OM:OC_{I-A}$	Change (%)	$\overline{OS}_{C\,(I-A)}$	Absolute Change
(Aiken et al., 2009)	0.53	32	1.82	12	1.86	11	-0.77	0.06
(Docherty et al., 2011)	0.44	27	1.71	10	1.73	9	-0.82	0.03
(Chen et al., 2009 and 2014)	0.60	34	1.65	14	1.94	13	-0.44	0.11
(Ge et al., 2012)	0.35	30	1.75	10	1.63	8	-1.05	0.00
(Gong et al., 2012)	0.50	26	1.63	9	1.87	9	-0.62	0.07
(He et al., 2011)	0.39	31	1.83	12	1.71	9	-1.04	-0.01
(Wang et al., 2010)	0.41	26	1.63	9	1.69	8	-0.80	0.03
(Huang et al., 2011)	0.60	27	1.64	11	1.94	11	-0.44	0.10
(Huang et al., 2012)	0.40	28	1.92	11	1.69	8	-1.13	-0.02
(Huang et al., 2013) (Winter)	0.43	30	1.73	11	1.75	9	-0.87	0.03
(Huang et al., 2013) (Summer)	0.36	28	1.94	10	1.67	8	-1.22	-0.02
(Martin et al., 2008)	0.69	26	1.40	11	2.04	11	-0.01	0.15
(Mohr et al., 2012)	0.41	30	1.77	11	1.70	9	-0.94	0.01
(Ovadnevaite et al., 2011)	0.70	17	1.34	8	2.05	8	0.06	0.11
(Poulain et al., 2011) (Summer)	0.52	17	1.51	7	1.83	6	-0.47	0.05
(Poulain et al., 2011) (Autumn)	0.54	14	1.48	7	1.84	6	-0.40	0.04
(Poulain et al., 2011) (Winter)	0.53	16	1.48	7	1.83	6	-0.41	0.05
(Robinson et al., 2011)	0.71	45	1.62	20	2.08	18	-0.20	0.17
(Saarikoski et al., 2012)	0.59	26	1.64	10	1.92	10	-0.46	0.09
(Setyan et al., 2012)	0.56	28	1.53	11	1.88	10	-0.40	0.10
(Sun et al., 2011)	0.46	28	1.65	11	1.75	9	-0.73	0.04

Table S3. Comparison of different versions of the organic fragmentation waves that can be used for AMS analysis

	Frag_organic	
m/z	Default AMS Frag. Table Allan et al., (2004)	Hildebrandt Ruiz et al., (2014) Correction
1		**Hwave***frag_organic [18**]**
16	0.04*frag_organic [18]	0.04*frag_organic [18]
17	0.25*frag_organic [18]	0.25*frag_organic [18]
18	1*frag_organic [44]	1*frag_organic [44]

Supplementary Material:

Calculation of H^+/H_2O^+ for Organic Frag Wave in AMS fragmentation table.

The current treatment of water fragmentation does not account for the H-atoms which were bound to HO^+ and O^+ before fragmentation. The neglected mass from H-atoms is negligible when calculating organic aerosol mass concentrations. However, the neglected H^+ signal does affect oxidation state ($\overline{OS}_c$ ~ 2×O:C - H:C) calculations from current H:C and O:C AMS values. In particular, the $\overline{OS}_c$ values are not invariant with respect to hydration/dehydration processes as they should be; the oxidation state decreases with dehydration because the prescribed H/O ratio of water in the AMS analysis is less than 2. Here we calculate H^+/H_2O^+ that needs to be added to the standard organic fragmentation wave to obtain an H/O ratio of 2 in the total signal of H_2O determined by AMS data analysis. The addition of H^+ changes the organic H:C ratio calculated in elemental analysis of the organic aerosol (OA) and therefore the oxidation state ($\overline{OS}_c$) estimated from O:C and H:C ratios.

The ratio of H^+/H_2O^+ needed to add to the updated fragmentation table to keep $\overline{OS}_c$ constant upon (de-) hydration can be calculated as follows:

For any given time point, let:

$x = H^+/H_2O^+$

z = initial mass of H_2O^+, y = factor by which H_2O changes,

f_{OH} = OH^+/H_2O^+ = 0.25 and f_O = O^+/H_2O^+ =0.04

Accounting for the contribution of ^{18}O:

$f'_{OH} = 1.00205499 * f_{OH}$ and $f'_O = 1.00205499 * f_O$

mw_i =molecular weights

f_{cal}^{OC} , f_{cal}^{HC} = calibration factors for O:C and H:C

The Aiken-Ambient and Aiken-Explicit values are 0.75 and 0.91, respectively

The Improved-Ambient values are (See Equations 8 and 9) :

$0.75*(1.26-0.623*f_{CO2}+2.28*f_{CHO})$ for O/C

$0.91*(1.07+1.07*f_{CHO})$ for H:C

NOTE: f_{CO2} and f_{CHO} are calculated using the default organic fragmentation wave that does not include the H^+ fragment since inclusion of the H^+ fragment does not significantly affect the calculated organic mass.

Then:

$$moles\ of\ O = z \times \left(\frac{f'_O}{mw_O} + \frac{f'_{OH}}{mw_{OH}} + \frac{1}{mw_{H_2O}}\right)$$

$$moles\ of\ H = z \times \left(\frac{f'_{OH}}{mw_{OH}} + \frac{2}{mw_{H_2O}} + \frac{x}{mw_H}\right)$$

To simplify the equations, let $\frac{f'_O}{mw_O} + \frac{f'_{OH}}{mw_{OH}} + \frac{1}{mw_{H_2O}} = a$ and $\frac{f'_{OH}}{mw_{OH}} + \frac{2}{mw_{H_2O}} = b$

Then:

$moles\ of\ O = z \times a$ and $moles\ of\ H = z \times \left(b + \frac{x}{mw_H}\right)$

Keeping oxidation state constant when H_2O is changed by y:

$$\frac{2}{f_{cal}^{OC}} \times zay - \frac{1}{f_{cal}^{HC}} zy \times \left(b + \frac{x}{mw_H}\right) = \frac{2}{f_{cal}^{OC}} \times za - \frac{1}{f_{cal}^{HC}} z \times \left(b + \frac{x}{mw_H}\right)$$

Dividing by z and rearranging:

$$\frac{2}{f_{cal}^{OC}} \times a(y-1) = \frac{1}{f_{cal}^{HC}} \times \left(b + \frac{x}{mw_H}\right)(y-1)$$

Dividing by (y-1) and rearranging:

$$x = \left(\frac{2f_{cal}^{HC}}{f_{cal}^{OC}} \times a - b\right) \times mw_H$$

The calculated H^+/H_2O^+ ratio from the above equations can be directly incorporated into the AMS analysis frag_organic wave as shown in Table S3. The modified Frag_organic wave refers to HWave, which is a new wave that contains time varying values of the H^+/H_2O^+ ratios over the time period being analyzed. For the

Aiken-Ambient and Aiken Explicit methods, where the constant Aiken et al. (2008) values are used for f_{cal}^{OC} and f_{cal}^{HC}, the HWave is constant over time at a value of 0.05. For the Improved-Ambient method, the variations in f_{cal}^{OC} and f_{cal}^{HC} introduce a time variation in HWave.

Supplementary References

Aiken, A. C., Salcedo, D., Cubison, M. J., Huffman, J. A., DeCarlo, P. F., Ulbrich, I. M., Docherty, K. S., Sueper, D., Kimmel, J. R., Worsnop, D. R., Trimborn, A., Northway, M., Stone, E. A., Schauer, J. J., Volkamer, R. M., Fortner, E., de Foy, B., Wang, J., Laskin, A., Shutthanandan, V., Zheng, J., Zhang, R., Gaffney, J., Marley, N. A., Paredes-Miranda, G., Arnott, W. P., Molina, L. T., Sosa, G., and Jimenez, J. L.: Mexico City aerosol analysis during MILAGRO using high resolution aerosol mass spectrometry at the urban supersite (T0) - Part 1: Fine particle composition and organic source apportionment, Atmos. Chem. Phys., 9, 6633-6653, 10.5194/acp-9-6633-2009, 2009.

Allan, J. D., Coe, H., Bower, K. N., Alfarra, M. R., Delia, A. E., Jiménez, J. L., Middlebrook, A. M., Drewnick, F., Onasch, T. B., Canagaratna, M. R., Jayne, J. T., and Worsnop, D. R.: Technical note: Extraction of chemically resolved mass spectra from Aerodyne aerosol mass spectrometer data, J. Aerosol Sci., 35, 909-922, 2004.

Chen, Q., Farmer, D. K., Schneider, J., Zorn, S. R., Heald, C. L., Karl, T. G., Guenther, A., Allan, J. D., Robinson, N., Coe, H., Kimmel, J. R., Pauliquevis, T., Borrmann, S., Poschl, U., Andreae, M. O., Artaxo, P., Jimenez, J. L., and Martin, S. T.: Mass spectral characterization of submicron biogenic organic particles in the Amazon Basin, Geophys. Res. Lett., 36, L20806, 10.1029/2009gl039880, 2009.

Chen, Q.: Manuscript in Preparation, 2014.

DeCarlo, P. F., Ulbrich, I. M., Crounse, J., de Foy, B., Dunlea, E. J., Aiken, A. C., Knapp, D., Weinheimer, A. J., Campos, T., Wennberg, P. O., and Jimenez, J. L.: Investigation of the sources and processing of organic aerosol over the Central Mexican Plateau from aircraft measurements during MILAGRO, Atmos. Chem. Phys., 10, 5257-5280, 10.5194/acp-10-5257-2010, 2010.

Docherty, K. S., Aiken, A. C., Huffman, J. A., Ulbrich, I. M., DeCarlo, P. F., Sueper, D., Worsnop, D. R., Snyder, D. C., Peltier, R. E., Weber, R. J., Grover, B. D., Eatough, D. J., Williams, B. J., Goldstein, A. H., Ziemann, P. J., and Jimenez, J. L.: The 2005 Study of Organic Aerosols at Riverside (SOAR-1): instrumental intercomparisons and fine particle composition, Atmos. Chem. Phys., 11, 12387-12420, 10.5194/acp-11-12387-2011, 2011.

Ge, X. L., Setyan, A., Sun, Y. L., and Zhang, Q.: Primary and secondary organic aerosols in Fresno, California during wintertime: Results from high resolution aerosol mass spectrometry, J. Geophys. Res., 117, D19301, 10.1029/2012jd018026, 2012.

Gong, Z., Lan, Z., Xue, L., Zeng, L., He, L., and Huang, X.: Characterization of submicron aerosols in the urban outflow of the central Pearl River Delta region of China, Frontiers of Environmental Science & Engineering, 6, 725-733, 10.1007/s11783-012-0441-8, 2012.

He, L. Y., Huang, X. F., Xue, L., Hu, M., Lin, Y., Zheng, J., Zhang, R. Y., and Zhang, Y. H.: Submicron aerosol analysis and organic source apportionment in an urban atmosphere in Pearl River Delta of China using high-resolution aerosol mass spectrometry, J. Geophys. Res., 116, D12304, Doi 10.1029/2010jd014566, 2011.

Hildebrandt Ruiz, L., et al. : Manuscript in preparation, 2014.

Huang, X. F., He, L. Y., Hu, M., Canagaratna, M. R., Kroll, J. H., Ng, N. L., Zhang, Y. H., Lin, Y., Xue, L., Sun, T. L., Liu, X. G., Shao, M., Jayne, J. T., and Worsnop, D. R.: Characterization of submicron aerosols at a rural site in Pearl River Delta of China using an Aerodyne High-Resolution Aerosol Mass Spectrometer, Atmos. Chem. Phys., 11, 1865-1877, DOI 10.5194/acp-11-1865-2011, 2011.

Huang, X. F., He, L. Y., Xue, L., Sun, T. L., Zeng, L. W., Gong, Z. H., Hu, M., and Zhu, T.: Highly time-resolved chemical characterization of atmospheric fine particles during 2010 Shanghai World Expo, Atmos. Chem. Phys., 12, 4897-4907, DOI 10.5194/acp-12-4897-2012, 2012.

Huang, X. F., Xue, L., Tian, X. D., Shao, W. W., Sun, T. L., Gong, Z. H., Ju, W. W., Jiang, B., Hu, M., and He, L. Y.: Highly time-resolved carbonaceous aerosol characterization in Yangtze River Delta of China: Composition, mixing state and secondary formation, Atmos. Environ., 64, 200-207, 10.1016/j.atmosenv.2012.09.059, 2013.

Martin, S. T., Rosenoern, T., Chen, Q., and Collins, D. R.: Phase changes of ambient particles in the Southern Great Plains of Oklahoma, Geophys. Res. Lett., 35, L22801, 10.1029/2008gl035650, 2008.

Mohr, C., DeCarlo, P. F., Heringa, M. F., Chirico, R., Slowik, J. G., Richter, R., Reche, C., Alastuey, A., Querol, X., Seco, R., Penuelas, J., Jimenez, J. L., Crippa, M., Zimmermann, R., Baltensperger, U., and Prevot, A. S. H.: Identification and quantification of organic aerosol from cooking and other sources in Barcelona using aerosol mass spectrometer data, Atmos. Chem. Phys., 12, 1649-1665, 10.5194/acp-12-1649-2012, 2012.

Ovadnevaite, J., O'Dowd, C., Dall'Osto, M., Ceburnis, D., Worsnop, D. R., and Berresheim, H.: Detecting high contributions of primary organic matter to marine aerosol: A case study, Geophys. Res. Lett., 38, L02807, 10.1029/2010gl046083, 2011.

Poulain, L., Spindler, G., Birmili, W., Plass-Dulmer, C., Wiedensohler, A., and Herrmann, H.: Seasonal and diurnal variations of particulate nitrate and organic matter at the IfT research station Melpitz, Atmos. Chem. Phys., 11, 12579-12599, 10.5194/acp-11-12579-2011, 2011.

Robinson, N. H., Hamilton, J. F., Allan, J. D., Langford, B., Oram, D. E., Chen, Q., Docherty, K., Farmer, D. K., Jimenez, J. L., Ward, M. W., Hewitt, C. N., Barley, M. H., Jenkin, M. E., Rickard, A. R., Martin, S. T., McFiggans, G., and Coe, H.: Evidence for a significant proportion of secondary organic aerosol from isoprene above a maritime tropical forest, Atmos. Chem. Phys., 11, 1039-1050, 10.5194/acp-11-1039-2011, 2011.

Saarikoski, S., Carbone, S., Decesari, S., Giulianelli, L., Angelini, F., Canagaratna, M., Ng, N. L., Trimborn, A., Facchini, M. C., Fuzzi, S., Hillamo, R., and Worsnop, D.: Chemical characterization of springtime submicrometer aerosol in Po Valley, Italy, Atmos. Chem. Phys., 12, 8401-8421, 10.5194/acp-12-8401-2012, 2012.

Setyan, A., Zhang, Q., Merkel, M., Knighton, W. B., Sun, Y., Song, C., Shilling, J. E., Onasch, T. B., Herndon, S. C., Worsnop, D. R., Fast, J. D., Zaveri, R. A., Berg, L. K., Wiedensohler, A., Flowers, B. A., Dubey, M. K., and Subramanian, R.: Characterization of submicron particles influenced by mixed biogenic and anthropogenic emissions using high-resolution aerosol mass spectrometry: results from CARES, Atmos. Chem. Phys., 12, 8131-8156, 10.5194/acp-12-8131-2012, 2012.

Sun, Y. L., Zhang, Q., Schwab, J. J., Demerjian, K. L., Chen, W. N., Bae, M. S., Hung, H. M., Hogrefe, O., Frank, B., Rattigan, O. V., and Lin, Y. C.: Characterization of the sources and processes of organic and inorganic aerosols in New York city with a high-resolution time-of-flight aerosol mass apectrometer, Atmos. Chem. Phys., 11, 1581-1602, 10.5194/acp-11-1581-2011, 2011.

Wang, X. F., Gao, S., Yang, X., Chen, H., Chen, J. M., Zhuang, G. S., Surratt, J. D., Chan, M. N., and Seinfeld, J. H.: Evidence for High Molecular Weight Nitrogen-Containing Organic Salts in Urban Aerosols, Environ. Sci. Technol., 44, 4441-4446, 10.1021/es1001117, 2010.